Supplementary Information:

Damping pathways of mid-infrared plasmons in graphene nanostructures

Hugen Yan[1†], Tony Low[1†], Wenjuan Zhu[1], Yanqing Wu[1], Marcus Freitag[1],

Xuesong Li[1], Francisco Guinea[2], Phaedon Avouris[1] and Fengnian Xia[1]

[1] *IBM T.J. Watson Research Center,*

Yorktown Heights, NY 10598, USA

[2] *Instituto de Ciencia de Materiales de Madrid. CSIC.*

Sor Juana Inés de la Cruz 3. 28049 Madrid, Spain

[†]*These authors contributed equally to this work*

I.   CALCULATING THE RPA DIELECTRIC FUNCTION AND LOSS FUNCTION

This section describes the modeling of the loss function in graphene on SiO_2 as shown in the intensity plot of Fig. 3b in the main manuscript.

A.   Intrinsic phonons

The only intrinsic phonons with momenta and energies similar to the graphene plasmons in our experiment are the longitudinal/transverse optical (LO/TO) phonons near the Γ point, with energies $\hbar\omega_{op} \approx 0.2\,\text{eV}$. On symmetry grounds[1], their coupling to electrons can be written as[2, 3]

$$\mathcal{H}_{e\text{-}op}(\mathbf{r}) = g_0 \begin{pmatrix} 0 & u_y(\mathbf{r}) + iu_x(\mathbf{r}) \\ u_y(\mathbf{r}) - iu_x(\mathbf{r}) & 0 \end{pmatrix} = \frac{g_0}{v_F}\hat{\mathbf{j}}(\mathbf{r}) \times \mathbf{u}(\mathbf{r}) \tag{1}$$

where v_F is the Fermi velocity and g_0 the coupling constant. The coupling constant can be estimated from the change with bond length of the hopping between nearest neighbor carbon π orbitals[4, 5], $g_0 \approx \partial t/\partial l$. The electronic Hamiltonian is described within each valley (and spin) in terms of the amplitudes on A/B sublattices, $\hat{\mathbf{j}}(\mathbf{r})$ is the single-particle current operator and $\mathbf{u}(\mathbf{r})$ is the relative displacement of the two sublattices. Their representation in terms of electron and phonon ladder operators, i.e. $\hat{a}_{\mathbf{k}}$ and $\hat{b}_{\mathbf{q}}$ respectively, are given by,

$$\hat{\mathbf{j}}(\mathbf{r}) = \frac{1}{A}\sum_{\mathbf{kq}} v_F \hat{a}_{\mathbf{k}}^\dagger \hat{\sigma} \hat{a}_{\mathbf{k+q}} e^{i\mathbf{q}\cdot\mathbf{r}} \equiv \frac{1}{A}\sum_{\mathbf{q}} \hat{\mathbf{j}}_{\mathbf{q}} e^{i\mathbf{q}\cdot\mathbf{r}} \tag{2}$$

$$\mathbf{u}(\mathbf{r}) = \sqrt{\frac{\hbar}{2\rho_m A\omega_{op}}} \sum_{\mathbf{q}\lambda} (\hat{b}_{\mathbf{q}\lambda} + \hat{b}_{-\mathbf{q}\lambda}^\dagger)\mathbf{e}_{\mathbf{q}\lambda} e^{i\mathbf{q}\cdot\mathbf{r}} \tag{3}$$

where $\hat{\sigma}$ are the Pauli spin matrices and $\mathbf{e}_{\mathbf{q}\lambda}$ are the polarization vectors. λ denotes the phonon modes, ρ_m is the mass density of graphene and A is its area. Using standard perturbation techniques, the effective electron-electron interaction mediated by optical phonons can be written as,

$$\mathcal{V}_{el\text{-}el}^{op} = \frac{1}{A^2}\sum_{\mathbf{q}\lambda} \frac{1}{v_F^2} |M_{op}|^2 \mathcal{D}_\lambda^0(\omega)\hat{\mathbf{j}}_{\mathbf{q}} \cdot \hat{\mathbf{j}}_{-\mathbf{q}} \equiv \frac{1}{A^2}\sum_{\mathbf{q}\lambda} v_{op,\lambda}\hat{\mathbf{j}}_{\mathbf{q}} \cdot \hat{\mathbf{j}}_{-\mathbf{q}} \tag{4}$$

where the scattering matrix elements and the free phonon Green's function are

$$|M_{op}|^2 = \frac{\hbar g_0^2}{2\rho_m \omega_{op}} \quad , \quad \mathcal{D}_\lambda^0(\omega) = \frac{2\omega_{op}}{\hbar((\omega + i\hbar/\tau_{op})^2 - \omega_{op}^2)} \tag{5}$$

where τ_{op} phenomenologically describes the phonon lifetime.

B. Surface polar phonons

Polar substrates, such as SiO_2 and BN have optical piezoelectric modes at energies $\hbar\omega_{sp}$. These modes induce electric fields which couple to the carriers in graphene[6, 7]. At long wavelengths, the effect of these can be described in terms of the dielectric function of the substrate,

$$\mathcal{H}_{e\text{-}sp} = \frac{1}{A} \sum_{\mathbf{kq}} M_{sp} \hat{a}^\dagger_{\mathbf{k+q}} \hat{a}_{\mathbf{k}} (\hat{b}_{\mathbf{q}\lambda} + \hat{b}^\dagger_{-\mathbf{q}\lambda}) \qquad (6)$$

with the scattering matrix elements defined as,

$$|M_{sp}|^2 = \frac{\pi e^2}{\epsilon_0} \frac{e^{-2qz_0}}{q} \mathcal{F}^2 \quad , \quad \mathcal{F}^2 = \frac{\hbar\omega_{sp}}{2\pi} \left(\frac{1}{\epsilon_{high} + \epsilon_{env}} - \frac{1}{\epsilon_{low} + \epsilon_{env}} \right) \qquad (7)$$

where z_0 is the graphene-substrate separation, $\mathcal{F}^2$ describes the Fröhlich coupling strength, ϵ_{low} (ϵ_{high}) are the low (high) frequency dielectric constant of the dielectric and ϵ_{env} is that of the environment. The effective electron-electron interaction mediated by surface optical phonons calculated from standard perturbation techniques yields[8],

$$\mathcal{V}^{sp}_{el\text{-}el} = \frac{1}{A^2} \sum_{\mathbf{q}\lambda} |M_{sp}|^2 \mathcal{D}^0_\lambda(\omega) \hat{\rho}_{\mathbf{q}} \hat{\rho}_{-\mathbf{q}} \equiv \frac{1}{A^2} \sum_{\mathbf{q}\lambda} v_{sp,\lambda} \hat{\rho}_{\mathbf{q}} \hat{\rho}_{-\mathbf{q}} \qquad (8)$$

where $\hat{\rho}_{\mathbf{q}} \equiv \sum_{\mathbf{k}} \hat{a}^\dagger_{\mathbf{k}} \hat{a}_{\mathbf{k+q}}$ and $\mathcal{D}^0_\lambda(\omega)$ contains also a phenomenological phonon lifetime of τ_{sp}.

C. Dielectric response

The plasmon response of graphene begins with finding the dielectric function. A satisfactory approximation can be obtained by adding the separate contributions *independently*. An effective interaction between electrons is given by the sum of the direct Coulomb interaction $v_c(q) = e^2/2q\epsilon_0$ and the two electrons interaction mediated by surface phonon $v_{sp,\lambda}(q,\omega)$. The RPA expansion of the dielectric function, $\epsilon^{rpa}_T(q,\omega)$, can be expressed with this effective interaction[9, 10]

$$v_{eff}(q,\omega) = \frac{v_c(q)}{\epsilon^{rpa}_T(q,\omega)} = \frac{v_c(q) + \sum_\lambda v_{sp,\lambda}}{1 - [v_c(q) + \sum_\lambda v_{sp,\lambda}] \Pi^0_{\rho,\rho}(q,\omega)} \qquad (9)$$

where $\Pi^0_{\rho,\rho}(q,\omega)$ is the non-interacting part (i.e. the pair bubble diagram) of the charge-charge correlation function given by a modified Lindhard function[11, 12],

$$\Pi^0_{\rho,\rho}(q,\omega) = -\frac{g_s}{(2\pi)^2} \sum_{nn'} \int_{BZ} d\mathbf{k} \frac{n_F(\xi_{\mathbf{k}}) - n_F(\xi_{\mathbf{k+q}})}{\xi_{\mathbf{k}} - \xi_{\mathbf{k+q}} + \hbar\omega + i\hbar/\tau_e} F_{nn'}(\mathbf{k}, \mathbf{q}) \qquad (10)$$

where $n_F(\xi_\mathbf{k})$ is the Fermi-Dirac distribution function, $F_{nn'}(\mathbf{k}, \mathbf{q})$ is the band overlap function of Dirac spectrum and τ_e is the lifetime of electrons. While the polar surface phonons couple to the charge density operator, the intrinsic optical phonon couple instead to the current operator. Its contribution to the dielectric function is given by $v_{op}(q, \omega)\Pi^0_{j,j}(q, \omega)$, where $\Pi^0_{j,j}(q, \omega)$ is the current-current correlation function. We note that from the usual charge continuity equation, $i\partial_t\hat{\rho}_\mathbf{q} = \mathbf{q} \cdot \hat{\mathbf{j}}_\mathbf{q}$, it follows that,

$$q^2\Pi_{j,j}(q, \omega) = \omega^2\Pi_{\rho,\rho}(q, \omega) - v_F\left\langle\left[\mathbf{q} \cdot \hat{\mathbf{j}}_\mathbf{q}, \hat{\rho}_{-\mathbf{q}}\right]\right\rangle \qquad (11)$$

where the second term in Eq. 11 is purely real and $\propto q^2$ as calculated in Ref. [13]. The imaginary part of $\Pi_{j,j}(q, \omega)$ can be obtained just from $\Im[\frac{\omega^2}{q^2} \times \Pi_{\rho,\rho}(q, \omega)]$. Collective modes with self consistent oscillations of the carrier charge can be obtained from the zeros of the full dielectric function

$$\epsilon_T^{rpa}(q, \omega) = \epsilon_{env} - v_c\Pi^0_{\rho,\rho}(q, \omega) - \epsilon_{env}\sum_\lambda v_{sp,\lambda}\Pi^0_{\rho,\rho}(q, \omega) - \epsilon_{env}v_{op}\Pi^0_{j,j}(q, \omega) \qquad (12)$$

where ϵ_{env} is the dielectric constant of graphene's environment.

D. Loss function

Our spectroscopy experiments measure the extinction spectra defined as $Z \equiv -\delta T/T_0$ with $\delta T = T - T_0$, where T (T_0) is the measured transmission with (without) plasmon excitations. In the experiment, a superlattice of graphene ribbons of width W defines the momentum i.e. $q = \pi/(W - W_0)$. W_0 accounts for the difference between physical and electrical device's width. Varying the frequency of the incident light excitation, ω, polarized perpendicularly (and parallely) to the ribbon, allows one to quantify the extinction spectra $Z(q, \omega)$, as first demonstrated in Ref. [14]. Resonance peaks in $Z(q, \omega)$ corresponds to enhanced optical absorption by graphene originating from plasmon oscillations[14–16] and can best be described by,

$$Z(q, \omega) \sim -\Im\left[\frac{1}{\epsilon_T^{rpa}}\right] \qquad (13)$$

where the latter is known as the loss function, which describes the ability of the system to dissipate energy via plasmon excitations and can be calculated from Eq. 12.

Using the above theory, we plot the loss function in graphene on SiO_2 as shown in Fig. 3b of the main manuscript. The calculations include interactions with the intrinsic and SiO_2 substrate phonons. Graphene doping is assumed to be $E_f = -0.43\,\mathrm{eV}$ and an effective $\epsilon_{env} = 1.5$. The frequencies of the various phonon modes are assumed to be at $\omega_{op} = 1580\,\mathrm{cm}^{-1}$, $\omega_{sp1} = 806\,\mathrm{cm}^{-1}$ and $\omega_{sp2} = 1168\,\mathrm{cm}^{-1}$. The damping time used in those plots are $\tau_e = 0.1\,\mathrm{ps}$, $\tau_{op} = 70\,\mathrm{fs}$ and $\tau_{sp} = 1\,\mathrm{ps}$. The coupling parameters used are $g_0 = 7.7\,\mathrm{eV\mathring{A}^{-1}}$, $\mathcal{F}_{sp1}^2 = 0.2\,\mathrm{meV}$ and $\mathcal{F}_{sp2}^2 = 2\,\mathrm{meV}$. Note that another substrate phonon at $\omega_{op} = 460\,\mathrm{cm}^{-1}$ was not included in the calculation, given that our experiment data are far above that frequency.

II. CALCULATING LIFETIMES OF THE PLASMON AND COUPLED PLASMON-PHONON MODES

This section describes the modeling of the plasmon lifetime in graphene on DLC and SiO_2 as shown in Fig. 4a and 4c of the main manuscript.

In the above previous analysis, the damping mechanisms for the plasmons are not discussed. Exchange of energy and momentum during scattering of plasmons can bring it into the Landau damping regime, leading to finite damping. In fact, when the plasmon energy exceeds the optical phonon energy, it can decay into a phonon together with an electron-hole pair, in such a way that the total momentum is conserved. In a phenomenological way, this decay can be accounted for through the single particle excitations, which have a finite lifetime τ_e, when their energies exceed the optical phonon energy[17], for example. Damping related to scattering with the ribbon's edges and a background damping due to impurities in the bulk can also be incorporated in τ_e. Finite phonon lifetime, τ_{sp}, can also influence to plasmon damping in the coupled plasmon-phonon modes. Below, we present our description of plasmon damping in the presence and absence of coupling with the surface phonon modes.

We are interested in the regime where $\omega > v_F q$ and $E_f \gg \hbar\omega$. In this limit,

$$\Pi_{\rho,\rho}^0(q,\omega) \approx \frac{E_f q^2}{\pi \hbar^2 (\omega + i\delta_e)^2} \tag{14}$$

where δ_e is the single-particle related damping in graphene defined as $\delta_e \equiv 1/\tau_e$. In the

absence of substrate phonon interactions, such as the case of graphene on a DLC substrate, the plasmon frequency is simply $\omega = \omega_{pl} + i\delta_e$, where $\omega_{pl}^2 = q|E_f|e^2/2\pi\hbar^2\epsilon_0\epsilon_{env}$ and δ_e also corresponds to plasmon damping. Note that in the regime we are considering i.e. $\omega > v_F q$ and $E_f \gg \hbar\omega$, Landau damping is excluded. Guided by experiments, the plasmon hybridizes strongly with one of the surface phonon modes with $\omega_{sp} \approx 0.145\,\text{eV}$ on SiO_2 substrate. For $\omega > \omega_{sp}$, we can write a simpler dielectric function,

$$\epsilon_T^{rpa} \approx \epsilon_{env}\left[1 - \frac{\omega_{pl}(q)^2}{(\omega + i\delta_e)^2} - \frac{\tilde{\omega}_{sp}^2}{(\omega + i\delta_{sp})^2 - \omega_{sp}^2 + \tilde{\omega}_{sp}^2}\right] \quad , \quad \tilde{\omega}_{sp} \equiv \sqrt{\frac{4\pi}{\hbar}\omega_{sp}\mathcal{F}^2} \quad (15)$$

where δ_{sp} is the surface phonons damping rate defined as $\delta_{sp} \equiv 1/\tau_{sp}$. The frequencies of the coupled plasmon-phonon modes can be obtained by setting $\epsilon_T^{rpa} = 0$ i.e.,

$$\omega^4 + i2\omega^3(\delta_{sp} + \delta_e) - \omega^2(\omega_{sp}^2 + \omega_{pl}(q)^2) - i2\omega(\omega_{sp}^2\delta_e + \omega_{pl}(q)^2\delta_{sp}) + \omega_{pl}(q)^2(\omega_{sp}^2 - \tilde{\omega}_{sp}^2) = 0$$

$$(16)$$

which can be solved numerically. In the limit where $\delta_e = \delta_{sp} = 0$, it reduces to a simple biquadratic equation with coupled plasmon-phonon modes solutions given by,

$$\omega_\pm^2 = \frac{\omega_{pl}^2 + \omega_{sp}^2}{2} \pm \frac{\sqrt{(\omega_{pl}^2 + \omega_{sp}^2)^2 - 4\omega_{pl}^2(\omega_{sp}^2 - \tilde{\omega}_{sp}^2)}}{2} \quad (17)$$

In the general case where $\delta_e = \delta_{ph} \neq 0$, we solve for the coupled plasmon-phonon modes via Eq. 16 numerically. However, in the $q = 0$ limit, it can be shown by setting $\epsilon_T^{rpa} = 0$ in Eq. 15 that $\omega = \omega_{sp} - i\delta_{sp}$. Therefore, the lifetime of the plasmon with frequency in the vicinity of the surface phonon frequency is determined by the surface phonon lifetime instead.

In this work, we assume that τ_{sp} is constant, to be fitted to experiment. Here, we discuss model description of the electron lifetime τ_e. Including relevant scattering mechanisms in our experiments, τ_e is given by,

$$\tau_e(q,\omega) \approx \left[\tau_0^{-1} + \tau_{edge}(q)^{-1} + \tau_{ep}(\omega)^{-1}\right]^{-1} \quad (18)$$

where τ_0 describes a background damping due to scattering with impurities and $\tau_{edge}(q) \approx a/(W - W_0)^b$ is related to scattering off the ribbon edges. $\tau_0 \approx 85\,\text{fs}$ as measured from the Drude response of large area, unpatterned graphene. $a \approx 2 \times 10^6$, of the order of Fermi velocity and $b = 1$ as discussed in the main text. $\tau_{ep}(\omega)$ is electron lifetime due to scattering

with optical phonons. It is related to the electron self-energy Σ_{ep} via $\tau_{ep} = \hbar/2\Im[\Sigma_{ep}]$ given by[9],

$$\Sigma_{ep}(\omega) = -k_B T \sum_{\mathbf{q},\omega_\lambda} |M_{op}|^2 \mathcal{D}_\lambda(\omega_\lambda)^0 \mathcal{G}^0(\mathbf{k}_f + \mathbf{q}, \omega + \omega_\lambda) \tag{19}$$

where $\mathcal{G}^0$ is the electron Green function and $\mathbf{k}_f$ is the Fermi wavevector. According to density functional calculations, the imaginary part of Σ_{ep} can be approximated by[18],

$$\Im[\Sigma_{ep}(\omega)] = \gamma_0 |\hbar\omega + \hbar\omega_0 + E_f| \times \frac{1}{2}\left[\operatorname{erf}\left(\frac{\hbar\omega - \hbar\omega_0}{\Delta_{ph}}\right) + \operatorname{erf}\left(\frac{-\hbar\omega - \hbar\omega_0}{\Delta_{ph}}\right) + 2\right] \tag{20}$$

where γ_0 describes the effective e-ph coupling and Δ_{ph} accounts for various energy broadening effects such as the deviation from the Einstein phonon dispersion model. They are estimated to be $\gamma_0 \approx 0.018$ and $\Delta_{ph} \approx 50\,\mathrm{meV}$ from density function calculations[18].

As discussed previously, in the absence of interaction with the surface phonons, the plasmon lifetime is simply $\tau_e(q, \omega = \omega_{pl})$. In the presence of interaction with surface phonons, the plasmon lifetime for the plasmon-phonon coupled modes can be solved via Eq. 16 numerically, with $\delta_e \approx [\tau_e(q, \omega = \omega_{pl}(q))]^{-1}$. The computed plasmon damping rates or lifetimes on DLC and SiO_2 substrates are shown in Fig. 4a and 4c of the main manuscript. There, graphene doping of $E_f \sim -0.43\,\mathrm{eV}$ was found to yield the best-fit to the dispersions of the various plasmon modes obtained experimentally, and is also consistent with the observed Pauli blocking in optical measurement.

In Fig. 3b of the main manuscript, we modeled the RPA loss function in SiO_2. However, the electron lifetime there was simply assumed to be constant. In Fig. S1, we calculate again the RPA loss function in SiO_2, but this time including the electron damping δ_e which describes our experiment as detailed in this section. After the inclusion of a more accurate description of electron damping, we note that the loss function can capture very well the plasmon peak intensity evolution for the three hybrid plasmon-phonon branches as seen experimentally, featuring two anti-crossings and spectral weight transfer from the low frequency to high frequency plasmon branch (peak 3) with increasing q.

In Fig. 4c of the main manuscript, we modeled the plasmon lifetimes of ribbons on DLC and SiO_2 with an estimated doping of $E_f \sim -0.43\,\mathrm{eV}$. We discussed here the uncertainty

in E_f on the calculated plasmon lifetimes through τ_{ep}. In Fig. S2, we plot the calculated plasmon lifetimes of ribbons on DLC and SiO$_2$ for dopings i.e. $E_f \sim -0.3\,\text{eV}$ and $-0.5\,\text{eV}$, which represents conservative upper and lower bounds in the uncertainty of our estimation of E_f. As shown in Fig. S2, doping have little effect on the DLC case, since damping is dominated mainly by edge scattering. The calculated plasmon lifetimes on SiO$_2$, although more sensitive to doping, varies only on the order of 10% for $\omega \gg \omega_0$ within the range of uncertainty in E_f.

In principle, plasmons can also decay via emission of surface polar phonons from the SiO$_2$ substrate. Here we discuss their their possible contributions from the surface polar phonons. As detailed above, the damping of the coupled plasmon-phonon mode is modeled by the respective lifetimes of their single particle excitations i.e. electrons and surface phonons, and their relative contributions depends on the plasmon-phonon character of that particular mode. For example, when the excitation frequency approaches that of the surface optical phonons, it excites a "phonon polariton" whose lifetime is determined by its phonons lifetimes. On the other hand, at excitation frequencies far from the surface optical phonons, it excites a "plasmon polariton" whose lifetime is determined by its electron lifetime. In our analysis of the plasmon losses, we mainly focus on a particular coupled plasmon-phonon mode, i.e. 3rd peak in Figure 3b of main manuscript, whose experimental lifetimes (fitted to theoretical ones) are plotted in Figure 4c of main manuscript. At frequencies much larger than ω_{sp2}, inelastic scattering of electrons with the second polar optical phonon mode is an intraband process which entails large momentum q transfer. Since the scattering matrix element goes as $1/q$, this process will therefore be greatly suppressed. Although scattering with the first polar optical phonon mode has a more favorable scattering phase space due to its lower energy, its Froihlich coupling strength is much weaker. As a result, inelastic scattering with optical phonons dominates the lifetime of this particular coupled plasmon-phonon mode at frequencies much larger than ω_{sp2}. Of course, at frequencies in the vicinity of ω_{sp2}, losses is determined by the polar phonons lifetimes instead. The other two coupled plasmon-phonon modes, i.e. 1st and 2nd peak in Figure 3b of main manuscript, located at frequencies near the surface polar phonon modes are phonon polaritons which exhibits long lifetime. Away from these phonon frequencies, their experimental resonance intensities are too weak to extract any meaningful information about their lifetime. Based on these

arguments, the plasmon losses via the interaction with surface polar phonons are relatively small in the frequency regions we focus and we neglected this effect in the main manuscript.

III.   RESONANCE LINESHAPE AND THE EXTRACTION OF THE PLASMON DAMPING

This section describes the extraction of the plasmon damping rate from the measured extinction spectra, used for Fig. 4 of the main manuscript.

The far-IR plasmon resonace lineshape of graphene micro-disks and ribbons can be well described by a damped oscillator model[19], which is derived from Drude conductivity. In the mid-IR regime, the lineshape becomes asymmetric, as seen for the third peak in Fig. 3a of the main manuscript. Because the lineshape of the resonance peaks in the vicinity of the substrate phonon frequencies might be affected by the plasmon-phonon hybridization, here we focus on the third peak of relatively narrow ribbons on SiO_2 substrate, whose resonance frequency is far away from those of substrate phonons. Fig. S3 shows a spectrum (black curve) of a ribbon array with width $W = 85$ nm. The spectrum is very asymmetric and a Fano resonance model[20, 21] can well describe it, as shown by the red curve in the figure. In the Fano framework, the extinction spectrum is expressed as

$$1 - \frac{T_{per}}{T_{//}} = \frac{2p}{\pi\Gamma_p(1 + q_f^2)} \frac{(q_f + \eta)^2}{(1 + \eta^2)} \qquad (21)$$

where p is a parameter for the amplitude, q_f is the Fano parameter, Γ_p is the plasmon damping rate, and $\eta = 2(\omega - \omega_0)/\Gamma_p$ with ω_0 being the center frequency. This equation is used to fit the spectra shown in the main manuscript to extract the plasmon damping rate Γ_p. Typical values for Fano parameter q_f are around 3.

This Fano type resonance indicates that the plasmon resonance is interfered by a broad background continuum. As demonstrated before, the optical conductivity of graphene in the far-IR is Drude like. However, in the mid-IR range we are dealing with here, it's in the Pauli blocking regime, i.e., the optical conductivity has a very weak Drude response tail and some residue conductivity due to many-body effect. It is this residue conductivity serving as the broad continuum to form a Fano type resonance with the plasmon excitation.

IV.   RESONANCE BROADENING EFFECT DUE TO THE RIBBON WIDTH INHOMOGENEITY

Long wavelength variations in the ribbon's width can also lead to an apparent resonance broadening effect indistinguishable from lifetime broadening effects. In DLC ribbons, the plasmon dispersion is described by a simple $\omega_{pl}^2 = \alpha q$ dispersion, where $\alpha \equiv |E_f|e^2/2\pi\hbar^2\epsilon_0\epsilon_{env}$. In this case, the resonance broadening $\delta\omega_{pl}$ associated with a characteristic width inhomogeneity of Δ is given by,

$$\delta\omega_{pl} \approx \frac{\sqrt{\alpha}\Delta}{2W_e^{\frac{3}{2}}} \tag{22}$$

In comparison to the plasmon lifetime broadening due to scattering off the edges, it also has a power law behavior of the form a/W_e^b, the scaling exponent b in this case is $\frac{3}{2}$ instead of 1. Fig. S4 plots the experimentally extracted plasmon damping as a function of the effective width W_e for two different doping levels. Least-square-error fit to the data yields $b = 1.0$, indicating that the broadening is due to carrier scattering off the edges. Furthermore, as shown in Fig. S4, there is also no noticeable dependence on doping, where the width inhomogeneity effect would suggest otherwise.

[1] J. L. Mañes, Phys. Rev. B **76**, 045430 (2007).

[2] T. Ando, J. Phys. Soc. Jpn. **75**, 124701 (2006).

[3] K. Ishikawa and T. Ando, J. Phys. Soc. Jpn. **75**, 084713 (2006).

[4] A. H. Castro Neto and F. Guinea, Phys. Rev. B **75**, 045404 (2007).

[5] D. M. Basko, Phys. Rev. B **78**, 125418 (2008).

[6] S. Fratini and F. Guinea, Phys. Rev. B **77**, 195415 (2008).

[7] J. Schiefele, F. Sols, and F. Guinea, Phys. Rev. B **85**, 195420 (2012).

[8] H. Bruus and K. Flensberg, Many-body quantum theory in condensed matter physics, Oxford University Press (2004).

[9] G. D. Mahan, Many-particle physics, Springer (2000).

[10] E. H. Hwang, R. Sensarma, and S. Das Sarma, Phys. Rev. B **82**, 195406 (2010).

[11] B. Wunsch, T. Stauber, F. Sols, and F. Guinea, New Journ. Phys. **8**, 318 (2006).

[12] E. H. Hwang and S. D. Sarma, Phys. Rev. B **75**, 205418 (2007).

[13] J. Sabio, J. Nilsson, and A. H. C. Neto, Phys. Rev. B **78**, 075410 (2008).

[14] L. Ju, B. Geng, J. Horng, C. Girit, M. Martin, Z. Hao, H. A. Bechtel, X. Liang, A. Zettl, Y. R. Shen, et al., Nature Nano. **6**, 630 (2011).

[15] F. Koppens, D. E. Chang, and F. J. G. de Abajo, Nano Lett. **11**, 3370 (2011).

[16] A. Y. Nikitin, F. Guinea, F. J. Garcia-Vidal, and L. Martin-Moreno, Phys. Rev. B **85**, 081405(R) (2012).

[17] M. Jablan, H. Buljan, and M. Soljačić, Phys. Rev. B **80**, 245435 (2009).

[18] C. H. Park, F. Giustino, M. L. Cohen, and S. G. Louie, Phys. Rev. Lett. **99**, 086804 (2007).

[19] H. Yan, X. Li, B. Chandra, G. Tulevski, Y. Wu, M. Freitag, W. Zhu, P. Avouris, and F. Xia, Nature Nano **7**, 330 (2012).

[20] U. Fano, Phys. Rev. **124**, 1866 (1961).

[21] Z. Li, C. H. Lui, E. Cappelluti, L. Benfatto, K. F. Mak, G. L. Carr, J. Shan, and T. F. Heinz, Phys. Rev. Lett. **108**, 156801 (2012).
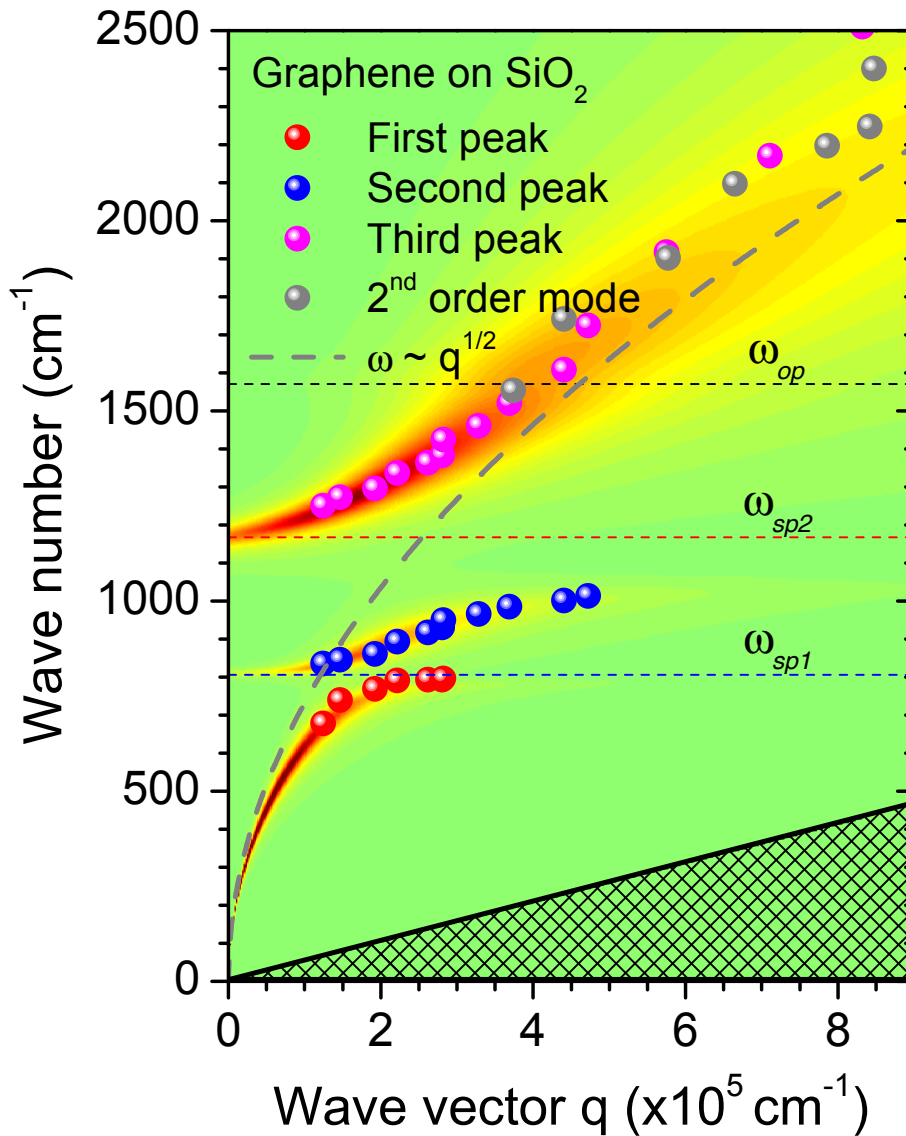
FIG. S 1: **Graphene loss function on SiO$_2$ substrate.** Calculated RPA loss function $\Im\left[1/\epsilon_T^{rpa}\right]$, including interactions with the intrinsic and SiO$_2$ substrate phonons. Graphene doping is assumed to be $E_f = -0.43\,\text{eV}$ and an effective $\epsilon_{env} = 1.5$. Shaded regions represent the intraband Landau damping regime i.e. $\hbar\omega/E_f < q/k_F$. Dashed line on the left plot is calculated from the classical plasmon dispersion $\omega_{pl}^2 = e^2 q v_F k_F/(2\pi\hbar\epsilon_0\epsilon_{env})$. The frequencies of the various phonon modes are assumed to be at $\omega_{op} = 1580\,\text{cm}^{-1}$, $\omega_{sp1} = 806\,\text{cm}^{-1}$ and $\omega_{sp2} = 1168\,\text{cm}^{-1}$. The lifetime associated with the phonons used in these plots are $\tau_{op} = 70\,\text{fs}$, $\tau_{sp1} = 0.5\,\text{ps}$ and $\tau_{sp1} = 0.2\,\text{ps}$. Calculations include damping of single particle excitations δ_e as described in the Suppl. info. text. The coupling parameters used are $g_0 = 7.7\,\text{eV\AA}^{-1}$, $\mathcal{F}_{sp1}^2 = 0.2\,\text{meV}$ and $\mathcal{F}_{sp2}^2 = 2\,\text{meV}$.
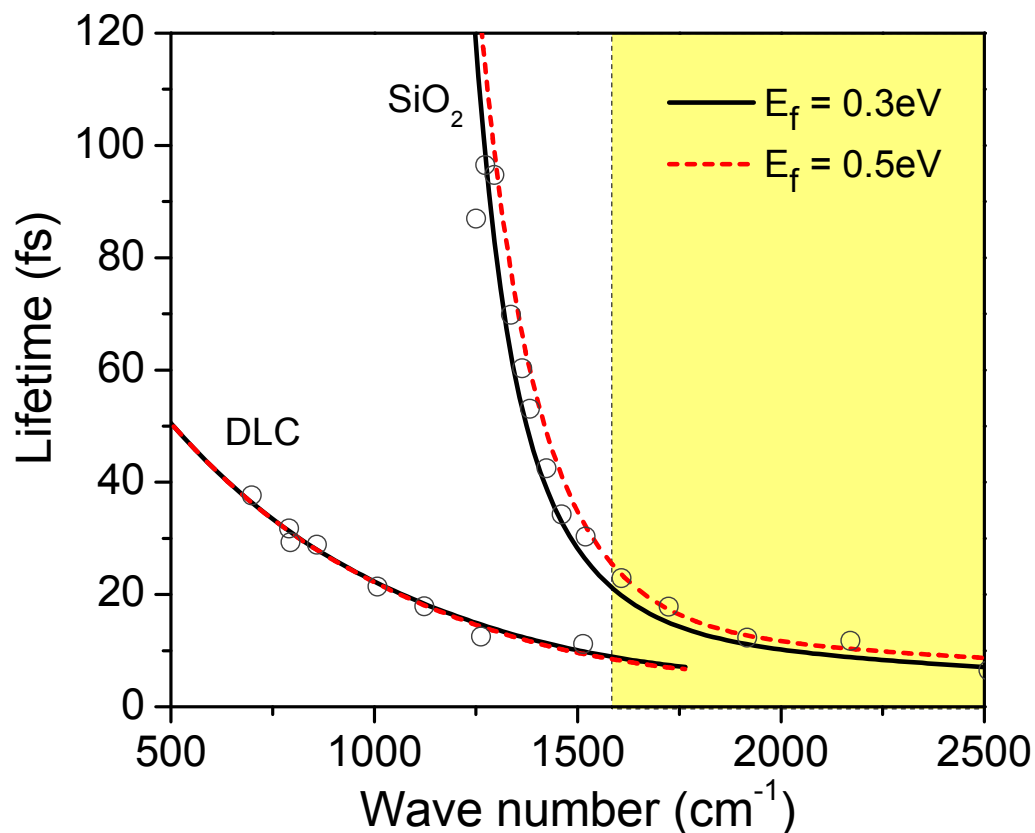
FIG. S 2: **Plasmon lifetimes with doping.** Calculated plasmon lifetimes of ribbons on DLC and SiO_2 as the function of the plasmon resonance frequencies with two different dopings as indicated. Calculations includes contributions from scattering with phonons, bulk scattering and edge scattering as detailed in the Supplementary Information. Symbols are experimental data. The yellow region represents the frequency range larger than the graphene optical phonon frequency.
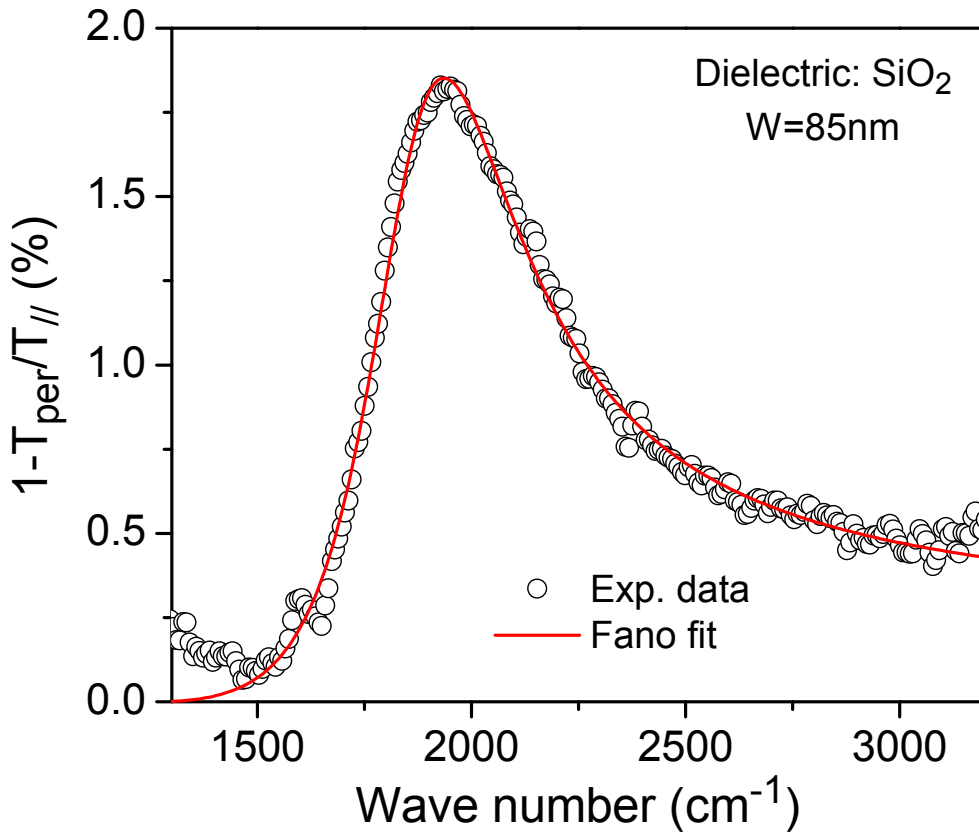
FIG. S 3: **Resonance lineshape and fitting.** Measured extinction spectra of a $W = 85\,nm$ ribbon array on SiO_2 substrate, where we show only part of the spectra relating to the peak 3 as described in the main manuscript. The data can be fitted well by a Fano model, with model and parameters described in Suppl. Info text.
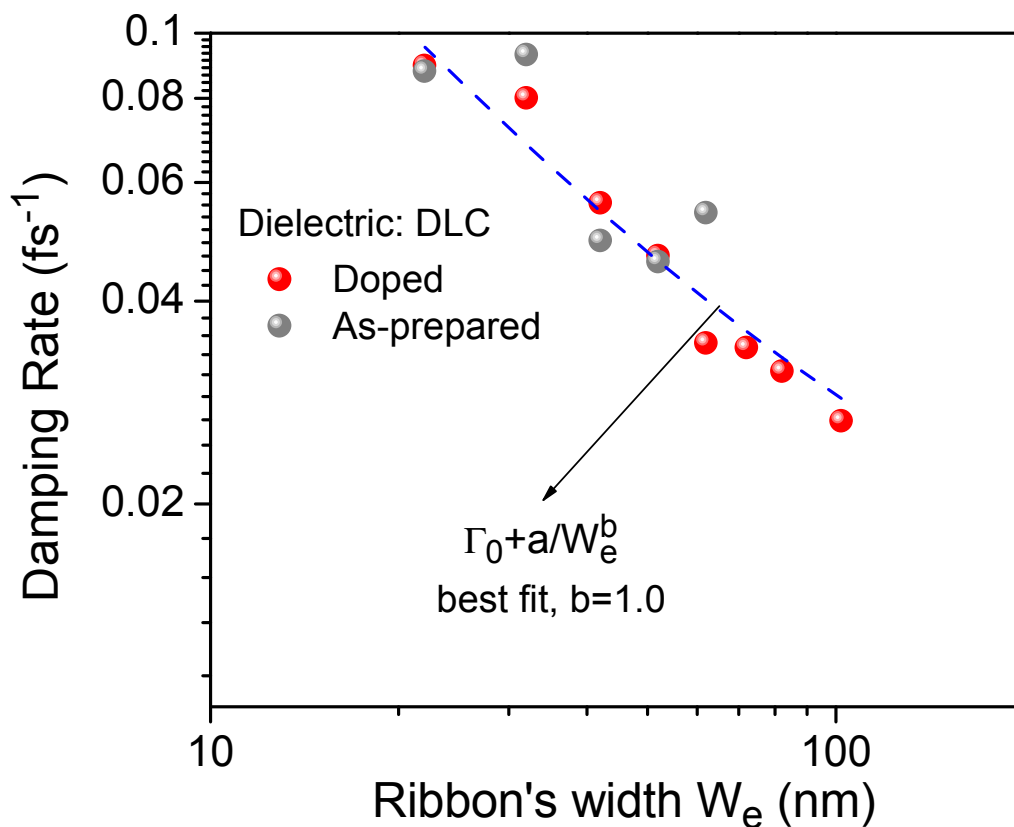
FIG. S 4: **Damping rate scaling with width.** Measured plasmon damping rate in graphene ribbons on DLC substrate as a function of the effective width $W_e = W - W_0$, where W is the physical width and $W_0 = 28\,nm$. See also main text. The plasmon damping rate is best described by the scaling relation $\Gamma_0 + a/W_e^b$, where $\Gamma_0 = 69cm^{-1}$ is related to the background damping, a quantity determined from the Drude response of large area graphene. a and b are obtained from least-square-error fit to the experimental data. b was found to be 1.0.